Development of a decay heat removal analysis code for the sodium-cooled fast reactor

Xiuli XUE[1], Hongyi Yang[1], Chao lin[1], Dalin Zhang[2]….

1. China Institute of Atomic Energy(CIAE), Beijing, China

2. Xi'an Jiao Tong University, Xi'an, China

E-mail contact of main author: M.A.Gonzalez-Espartero@iaea.org

Abstract: The decay heat removal capacity after emergency shutdown is one of the most important security indexes for sodium-cooled fast reactors. Dedicated decay heat removal system is in great need in analyzing the core decay heat removal capacity in designing sodium cooled fast reactor. In this paper, a decay heat removal analysis code in a unified development platform has been developed with modular programming, which contains the primary loop with components of core, inter-wrapper fluid and heat exchanger, as well as the decay heat removal loop with typical components in the sodium intermediate and air cooling circuit. Many studies have been conducted on code verification including international benchmark analysis and the comparison with the steady state of China Experimental Fast Reactor, which shows the results are in good agreement. Various kinds of transient calculation on the China Experimental Fast Reactor will be performed and the results will be compared with the experiments to validate the code further.

Keywords: Decay heat removal, Code development, Sodium-cooled fast reactor, inter-wrap flow

1 Introduction

Loss of flow and heat sink accident induced by blackout accident is one of the most serious accidents for sodium-cooled fast reactor, which will cause the risk of core damage without removing the decay heat effectively in time. Therefore, the decay heat removal capacity after emergency shutdown in sodium-cooled fast reactor is one of the most important safety indexes and has attracted wide attention. Therefore, generally decay heat removal system is designed to remove the decay heat and the core decay heat removal capacity is analyzed in emergency shutdown for sodium-cooled fast reactors.

Many countries have developed computer codes to calculate the reactor thermo-hydraulics in pool-type sodium-cooled fast reactor, including the RUBIN and GRIF in Russia, the OASIS and TRIO-U in France (Tenchine D. et al.,2012), the SAS4A in America (Cahalan and Wei, 1990; Cahalan et al.,1994;Fanning, T., 2012.) and so on. Generally, those codes aim at the whole system

analysis but not limited to decay heat removal condition. In China, researchers have also performed a lot of studies on the base of China Experimental Fast Reactor(CEFR). LIAO Zhijie et. al (1998) have developed a system analysis code to study the process of the decay heat removal in emergency shutdown for CEFR, and provided a reference for the safety operation in CEFR.

To support the development of sodium-cooled fast reactor in China, a decay heat removal analysis code for sodium-cooled fast reactor is being developed which contains the primary loop, as well as the decay heat removal loop including the sodium intermediate and air cooling circuit. This code has the ability of the parametric sensitivity analysis, optimal design of system, and evaluation of decay heat removal capacity. The primary functions of this code has been completed and is now at the state of optimization and verification.

2 Fundamental Models

The primary loop and decay heat removal system of typical pool-type sodium-cooled fast reactor is shown in Fig 1. In an emergency shutdown, the core and the inter-wrapper flow (IWF) will take the decay heat into the hot pool, which will be transferred further to the intermediate loop of the decay heat removal system by independent heat exchanger (DHX), and finally the decay heat will be taken away by the air heat exchanger (AHX) into the final heat sink i.e. air.

On the base of this kind of heat removal method, appropriate mathematical and physical models are adopted to describe the thermal-hydraulic characteristics of the primary loop and decay heat removal system in an emergency shutdown, and the code of decay heat removal analysis system is developed with reasonable program architecture and coding. As shown in Fig. 1, the components of the system contain core (inner and inter wrapper), cold pool, hot pool, IHX, AHX, DHX, pump, pipe, pipe net, reactor vessel cooling system (RVCS), pump support cooling system and so on. The thermal parameters of the IHX secondary side, the AHX air side, the core power and the initial value of the components should be offered in a calculation.

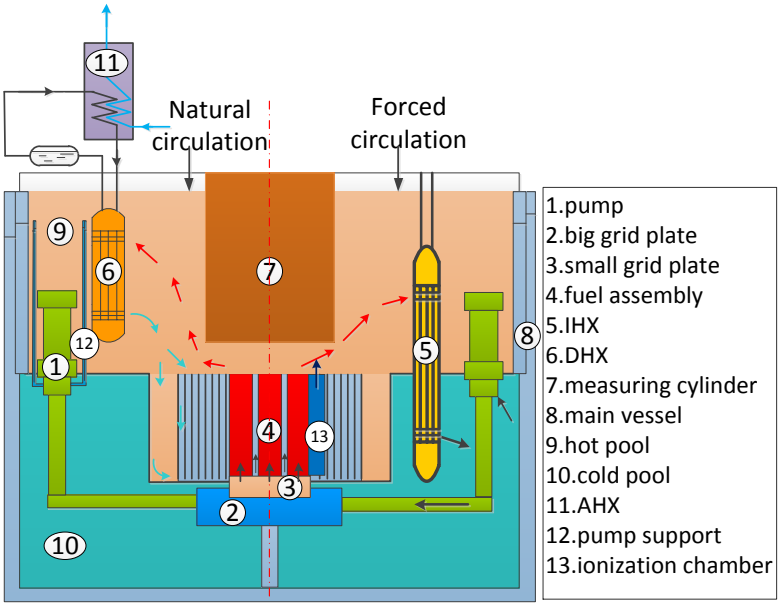

Fig. 1 Structure diagram of typical sodium cooled fast reactor

2.1 Core model

2.1.1 Sodium flow and heat transfer

The conservation of mass, energy and momentum for sodium flow in one dimension can be described as the following equation, in which the single liquid phase of sodium is assumed to be incompressible without considering the gravity and pressure effects.

$$\frac{\partial \rho}{\partial t}+\frac{\partial}{\partial z}\left(\frac{W}{A}\right)=0 \tag{1}$$

$$\frac{\partial}{\partial t}\left(\frac{W}{A}\right)+\frac{\partial}{\partial z}\left(\frac{W^2}{\rho A^2}\right)=-\frac{\partial p}{\partial z}-\frac{fW|W|}{2D_e\rho A^2}-\rho g \tag{2}$$

$$\rho\frac{\partial h}{\partial t}+\frac{W}{A}\frac{\partial h}{\partial z}=\frac{qU}{A} \tag{3}$$

2.1.2 Power generation

The fission power of core is proportional to neutron flux. Thus the change of the neutron flux along with time and space can be used to describe the fission power (Guppy, 1983). The point reactor kinetics model with six-group delayed neutrons can be applied to calculate the fission power, and the equations are shown as follows:

$$\frac{dn}{dt}=\frac{\rho-\beta}{\Lambda}n+\sum_{i=1}^{n_c}\lambda_i C_i \tag{4}$$

$$\frac{dC_i}{dt}=\frac{\beta_i}{\Lambda}n-\lambda_i C_i,\quad i=1,2,\ldots,\ n_c \tag{5}$$

The fission power is decided by the total reactivity which includes the external input reactivity and the intrinsic reactivity caused by the change of the core parameters. The total reactivity is as follows:

$$\rho(t)=\rho_a(t)+\sum\rho_i(t) \tag{6}$$

2.2 Inter-wrapper flow

In the IWF model, the inter-wrapper gaps are divided into several layers based on the layout of subassemblies, as shown in Fig. 2. The inter-wrapper gaps between the neighboring layers of subassemblies are considered as one layer of IWF. In Fig. 2, the inter-wrapper gaps located in the same layer are of the same color (i.e. the first layer and second layers are black and red, respectively).

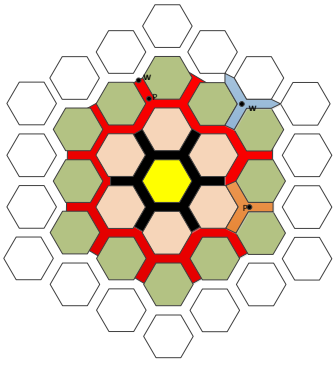

Fig. 2 The schematic diagram of radial layers in IWF

As the flow and heat transfer in the inter-wrapper gaps are complex, some basic assumptions are made as follows:

(1)The dissipated energy is little compared with the heat transfer from subassemblies, and it

is neglected.

(2) The heat conduction between two control volumes of IWF is so small that it is ignored(relative to the heat exchange between subassemblies and IWF).

(3) The flow in circumferential direction is ignored and the solution of IWF was simplified into a two-dimensional problem.

(4) Sodium is incompressible and the density of sodium is only a function of temperature.

Thus the governing equations (i.e. Mass continuity equation, Energy conservation equation, Axial and Transverse momentum conservation equation, respectively) in this model are derived from N-S equations (Tao, 2001), as shown below.

$$A_i \frac{\partial}{\partial t}\rho_i + \frac{\partial}{\partial z} m_i + \sum_{j\in i} w_{ij} = 0 . \tag{7}$$

$$A_i \frac{\partial \langle \rho h \rangle_i}{\partial t} + \frac{\partial m_i h_i}{\partial z} + \sum_{j\in i} h^* w_{ij} = \bar{q}_i - \sum_{j\in i} \frac{s_{ij}}{l_{ij}} K \left(T_i - T_j \right). \tag{8}$$

$$\frac{\partial m_i}{\partial t} + \frac{\partial m_i u_i}{\partial z} + A_i \frac{\partial p_i}{\partial z} = -g\rho_i A_i - \sum_{j\in i} u_i^* w_{ij} - \frac{1}{2}\left(\frac{f_i}{D_i} + \frac{K_s}{\Delta z} \right) \frac{m_i^2}{A_i \rho_i} . \tag{9}$$

$$\frac{\partial w_{ij}}{\partial t} + \frac{\partial \left(v_{ij} w_{ij} \right)}{\partial x} = \frac{S_{ij}}{l_{ij}} \left(p_i - p_j \right) - \sum_{j\in i} m_j^* v_{ij} - \frac{1}{2}\left(\frac{f_j}{D_j} + \frac{K_G}{\Delta x} \right) \frac{|w_{ij}| w_{ij}}{S_{ij} l_{ij} \rho^*} . \tag{10}$$

In the transverse momentum conservation equation, the pressure drops contain the frictional and resistance pressure drop (G.H.Su, 2013).

2.3 Main vessel cooling system

The control volume of the main components in RVCS is shown in Fig. 3. On the operation condition, cold sodium from the cold pool is pumped by the pump to flow upwards through the outer annulus and finally returns to the cold pool by flowing downwards in the inner annulus. However, the pump driving force will disappear and the fluid in RVCS may flow reversely under the natural circulation condition when accidents occur.

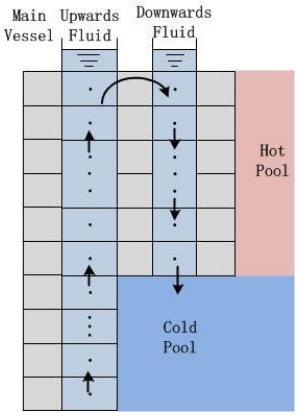

Fig. 3 Control Volumes of RVCS

In RVCS, the upwards and downwards fluids share the same argon space with the same pressure, therefore the height difference of liquid levels in the two channels determines the flow directions, normal or reverse. For the fluid in the annulus, the basic equations of mass, momentum and energy are:

$$\frac{dm_i}{dt} = W_{i,in} - W_{i,out} \tag{11}$$

$$\frac{l_i}{A_i}\frac{dW_i}{dt} = P_{i,in} - P_{i,out} - \Delta P_i \tag{12}$$

While the pressure difference of the two fluids at the same axial position caused by the height difference is related to the mass flow of the fluid:

$$\begin{aligned}\Delta p_c &= \frac{f_c W_c |W_c|}{2\rho_1 A_c^{\,2}} \\ &= P_{1,out} - P_{2,in}\end{aligned} \tag{13}$$

$$A_i\rho_i L_i \frac{\partial H_i}{\partial t} + W_i L_i \frac{\partial H_i}{\partial z} + H_i \frac{\partial m_i}{\partial t} = \Phi \tag{14}$$

2.4 Pool model

The temperature of the hot and cold pool is evenly distributed under operation condition, while thermal stratification (Chang et al., 2002) occurs under accident conditions. To simulate the thermal stratification in the pool, multi-grid method is performed which is similar to the large space fluid flow and heat transfer method in RELAP5, and the control volume is shown in Fig. 4. The radial control volume is connected by the nozzle to calculate the flow and heat transfer, while the energy and momentum conservation equation is taken into consideration in the main control volume. The governing equations are as follows:

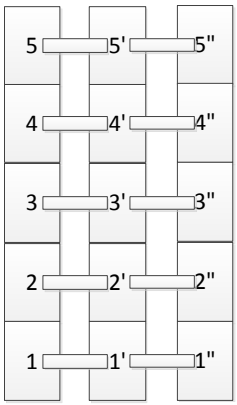

Fig. 4 Control Volumes of multi-grid pool

Radial momentum conservation equation： $$\frac{\partial w_{ij}}{\partial t} = A_{ij}\frac{\partial p_{ij}}{\partial x} - \frac{f_{ij}}{2}\frac{w_{ij}|w_{ij}|}{\rho A_{ij} D_{e,ij}} \tag{15}$$

Radial heat transfer equation： $$Q_{ij} = h_{jk} A_{ij} \frac{\partial T_{ij}}{\partial x} \tag{16}$$

Mass conservation equation： $$A_i \frac{\partial}{\partial t}\rho_i + \frac{\partial}{\partial z} m_i + \sum_{j\in i} w_{ij} = 0 \tag{17}$$

Axial momentum conservation equation： $$\frac{\partial \rho u_i}{\partial t} + \frac{\partial \rho u_i u_i}{\partial z} = -g\rho_i A_i - \frac{1}{2}\frac{f_i}{D_i}\frac{\rho u_i^2}{A_i} - A_i \frac{\partial p_i}{\partial z} \tag{18}$$

Energy conservation equation： $$\frac{\partial(\rho H)}{\partial t} + \frac{\partial}{\partial z}\left(\frac{WH}{A}\right) = \frac{Q}{A} + \frac{\partial P}{\partial t} \tag{19}$$

2.5 Na-Na heat exchanger

The Na-Na heat exchanger in this paper contains the inner heat exchanger and the independent heat exchanger (i.e. IHX and DHX), whose construction and model are almost the

same. To simulate the two-dimensional effects on the radial cross section, the heat exchanger tubes in the same circle are assumed to be one layer. The heat transfer between the neighboring layers is also taken into consideration in addition to the original one-dimensional governing equations.

$$A_f \rho_f c_{pf} \frac{\partial T_f}{\partial t} = -W_f c_{pf} \frac{\partial T_f}{\partial z} - U_f h_f (T_f - T_W) + \frac{1}{r} \frac{\partial}{\partial r} \left(k_f r \frac{\partial T_f}{\partial r} \right) \tag{20}$$

$$A_s \rho_s c_{ps} \frac{\partial T_s}{\partial t} = -W_s c_{ps} \frac{\partial T_s}{\partial z} + U_s h_s (T_W - T_s) \tag{21}$$

$$A_w \rho_w c_{pW} \frac{\partial T_W}{\partial t} = U_f h_f (T_f - T_w) - U_s h_s (T_W - T_s) \tag{22}$$

$$A_b \rho_b c_{pb} \frac{\partial T_b}{\partial t} = U_f h_f (T_f - T_b) - U_h h_h (T_h - T_b) \tag{23}$$

2.6 Na-Air heat exchanger

In the Na-Air heat exchanger (AHX), since the air specific heat, density and the heat-transfer coefficient are less than that of sodium, the volume of AHX is generally very large. The mathematical model in the sodium side is the same as IHX, which won't be explained again. One-dimensional single-tube model is applied in the heat transfer region in the air side, the basis equations are as follows:

$$W_{i+1} = W_i = W \tag{24}$$

$$\rho_i V_i \frac{dh_i}{dt} = W h_{i+1} - W h_i + q_i A_i \tag{25}$$

$$p_{i+1} = p_i - \left(\frac{W^2}{\rho_{i+1} A_{i+1}} - \frac{W^2}{\rho_i A_i}\right) - \rho_i g \Delta z_i - \frac{f_i W^2 \Delta z_i}{2 \rho_i D_e A^2} - \sum_{j=1}^{n} \left(\frac{f_l W^2}{2 \rho A^2} \right)_j \tag{26}$$

3 Numerical method and program development

3.1 Numerical method

All of the models developed above can be converted into the style of the ordinary differential equations, which will lead to a large initial value problem of the parameters:

$$\begin{cases} \dfrac{d\vec{y}}{dt} = f\left(t, y, y'\right) \\ \vec{y}(0) = \vec{y}_0 \end{cases} \tag{27}$$

The calculation shows that the adopted combination of Adams predictor-corrector method and Gear method (Gear, 1971), with IWF adopting SIMPLE and being coupled with Gear method, has obtained good results with high solving accuracy and fast computing speed.

3.2 Program structure and flow chart

This code employs the object-oriented modular modeling method with the property of good portability. As shown in Fig. 5, each component as one module has the similar construction and the main components contain core (inner and inter wrapper), cold pool, hot pool, IHX, AHX, DHX, pump, pipe, pipe net, RVCS. In addition to the components module, the input module, output module, coupling module, physical property, numerical computation module and auxiliary module are shared by the whole program.

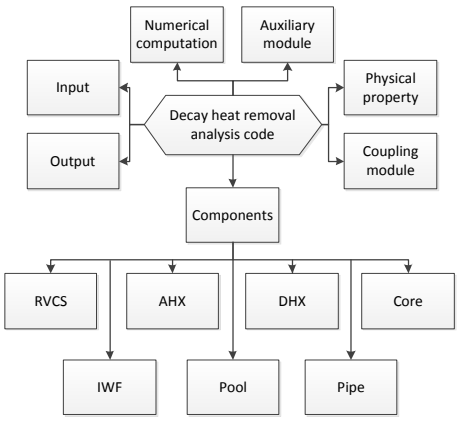

Fig. 5 Program structure

In this paper, the Gear method is adopted for the numerical integration of the differential equations. Based on the calculation method and content, the program flow includes the steady state calculation, transient calculation and the restart calculation as shown in Fig. 6.

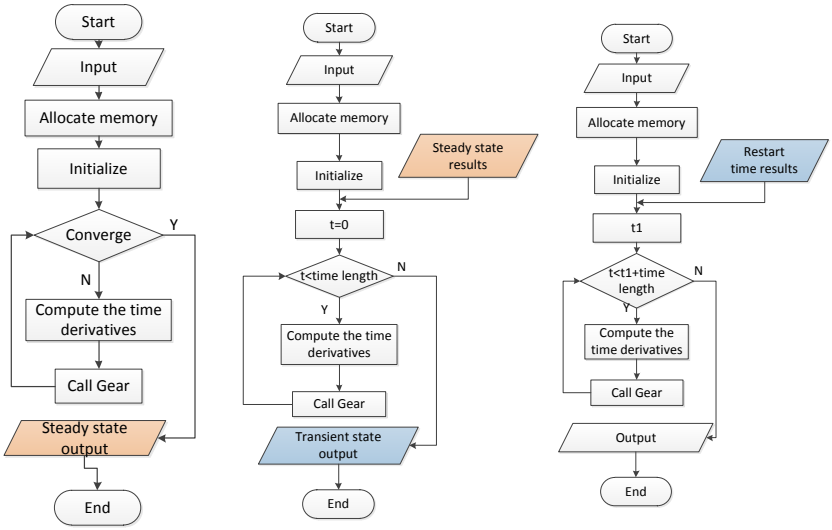

(a) Steady-state calculation (b) Transient calculation（c）Restart calculation

Fig. 6 Program flow chart

4 Preliminary verification

The one-dimensional code of decay heat removal analysis system will be verified with international benchmark and the design parameters and experimental data of CEFR. At the present stage, the international benchmark analysis and the comparison with the steady state of CEFR have been performed, which showed the results are in good agreement. Various kinds of transient calculation on CEFR are underway to verify the code further.

4.1 International benchmark—SHRT-17 for EBRII

4.1.1 Brief description of EBRII and SHRT-17

As shown in Fig. 7, EBR-II is a sodium-cooled fast reactor using metal fuel built by the Argonne National Laboratory(ANL), and it began operation in1964 and shut down in 1994. A series of shutdown heat removal tests were carried out from 1984 to 1986 to demonstrate its

inherent safety feature (Herzog et al., 1992). Two of the tests, i.e. SHRT-17 and SHRT-45R are being used as a benchmark in the IAEA project 'Benchmark Analyses of an EBR-II Shutdown Heat Removal Test'.

In the SHRT-17 test, the loss of flow accident was simulated with the trip of the primary coolant pumps, the auxiliary electro-magnetic pump and the immediate-loop pump. The plant protection system was put in use immediately with the full insertion of control rods at the test initiation (Sumner and Wei, 2012; Mohr et al., 1987; Yue N. et al., 2015). The variations of primary pump speeds, total power, intermediate IHX inlet sodium flow rate and temperature versus time were provided in the test as boundary conditions.

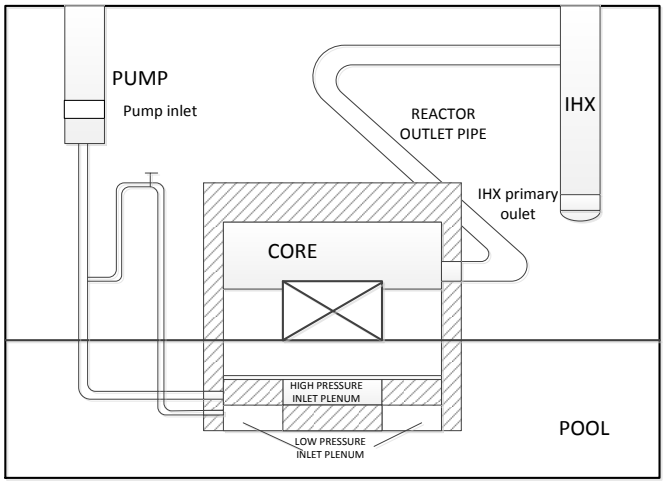

Fig. 7 Schematic of the primary system

4.1.2 Results and discussion

All the components, pipes and pool in the primary loop were constructed with the code developed in this paper to simulate the test. The comparison between the calculation values and experiment data of some typical parameters is shown in Fig. 8-Fig. 10.

Fig. 8 shows the variation of calculation and experiment data of the Z-Pipe inlet and IHX intermediate outlet temperature with time. It can be seen that the trends are coincident and the relative deviation of the peak value is within 10%.

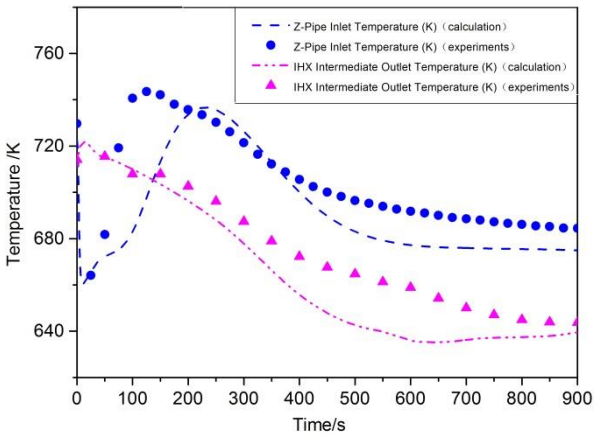

Fig. 8 Comparison between the calculation and experiment temperature

As shown in Fig. 9, the mass flow variation with time in XX09 agrees well with the experiment values. Not only can the code simulate the mass flow of the whole core under accident

condition accurately, but also predict the flow distribution.

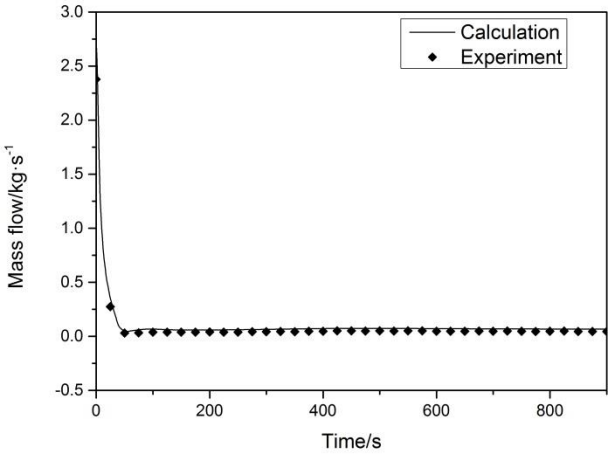

Fig. 9 Mass flow in XX09

The coolant temperature curve in different axial position of XX09 is shown in Fig. 10. The temperature in XX09 rises sharply, with the maximum at the top of core. As can be seen from Fig. 10, the calculation agrees well with the experimental data, with the peak temperature relative deviation of 2.6%.

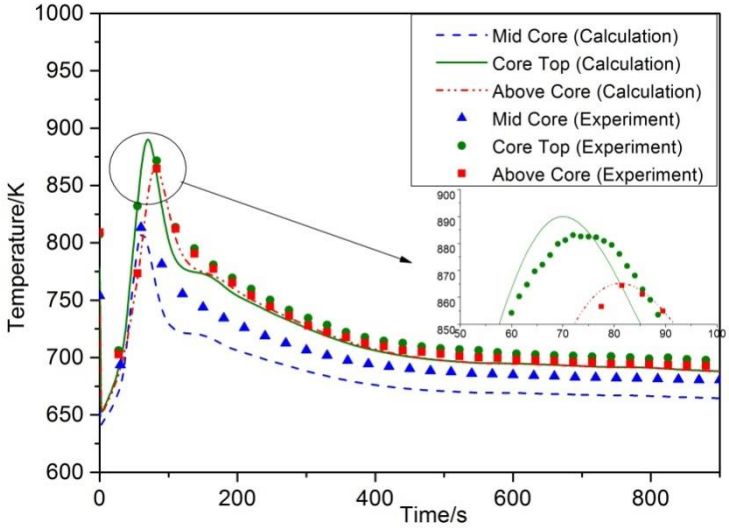

Fig. 10 The temperature in different axial position of XX09

4.2 The steady state calculation of CEFR

This paper has performed the steady state calculation of CEFR and the results are compared with the design values, which shows the results are in great agreement. Almost all the components of CEFR are taken into consideration in the simulation, and the difference values and the error with the design value of some typical parameters is showed below in Table 1.

Table 1 Difference and error with design value

Components	Parameter	Difference with design value	Error(/%)
CORE	Inlet temperature	3.51	0.974
	Outlet temperature	1.49	0.281
	Mass flow	-0.27	-0.090
IHX	Primary inlet temperature	-0.59	-0.115
	Primary outlet temperature	1.13	0.320

	Secondary outlet temperature	-2.08	-0.421
DHX	Secondary inlet temperature	-2.43	-0.501
	Secondary outlet temperature	-2.97	-0.577
AHX	Air outlet temperature	-0.67	-0.134
	Air mass flow	0.00	0.727
RVCS	Inlet temperature	3.51	0.974
	Outlet temperature	3.72	0.930
	Mass flow	-0.02	-0.048

5 Summary and Conclusion

The decay heat removal capacity after emergency shutdown is one of most important security indexes for sodium-cooled fast reactor. Dedicated decay heat removal system is in great need in analyzing the core decay heat removal capacity in designing sodium cooled fast reactor. A decay heat removal analysis code for typical pool-typed sodium cooled fast reactor has been developed in this paper. This code has the ability of the parametric sensitivity analysis, optimal design of system, and evaluation of decay heat removal capacity.

This paper presents the program structure, the numerical method and fundamental models containing the primary loop including components of core, inter-wrapper fluid, heat exchanger, as well as the decay heat removal loop with the typical components in the sodium intermediate and air cooling circuit. The international benchmark analysis and the comparison with the steady state of China Experimental Fast Reactor showed that the results are in good agreement. Various kinds of transient calculation on CEFR will be performed next and the results will be compared with the experimental data to verify the code further.

Reference

Cahalan J.E., Tentner A.M., Morris E.E., 1994. Advanced LMR safety analysis capabilities in the SASSYS-1 and SAS4A computer codes. Argonne National Lab., IL (United States). Funding organisation: USDOE, Washington, DC (United States).

Cahalan, J.E., Wei, T.Y.C., 1990. Modeling Developments for the SAS4A and SASSYS Computer Codes. Argonne National Lab, IL (USA).

Chang, W.P., Kwon, Y.M., Lee, Y.B., Hahn, D., 2002. Model development for analysis of the Korea advanced liquid metal reactor. Nuclear Engineering and Design 217, 63–80.

Fanning, T., 2012.The SAS4A/SASSYS-1 Safety analysis code system.ANL/NE-12/4, Nuclear Engineering Division, Argonne National Laboratory.

Gear, C.W., 1971. Numerical Initial Value Problems in Ordinary Differential Equation. Prentice-Hall, Englewood Cliffs, NJ.

G.H.Su, S.Q., Wenxi Tian,et al., 2013. Thermal Hydraulic Numerical Analysis of Nuclear Power System.

Guppy, J.G., 1983. System Code (SSC, Rev. 0), An Advanced Thermo hydraulic Simulation Code for Transients in LMFBRs. Brookhaven National Lab.

Herzog, J.P., Chang, L.K., Dean, E.M., Feldman, E.E., Hill, D.J., Mohr, D., Planchon, H.P., 1992. Code Validation with EBR-ii Test Data. Dynamics and Control in Nuclear Power Stations, p. 165 (Telford).

LIAO Zhijie, REN Yuxin, SHEN Mengyu, et al. Numerical Simulation of Decay Heat Removal in Fast-reactor in an Accident[J]. Journal of Basic Science and Engineering, 1998,0(1);59-64

Mohr, D., Chang, L.K., Feldman, E.E., Betten, P.R., Planchon, H.P., 1987. Loss-of-primary-flow-without-scram tests: pretest predictions and preliminary results. Nucl. Eng. Des. 101 (1), 45e56.

Sumner, T., Wei, T.Y.C., 2012. Benchmark Specifications and Data Requirements for EBR II Shutdown Heat Removal Tests SHRT 17 and SHRT 45R. Nuclear Engineering Division Argonne National Laboratory. ANL-ARC-226-(Rev 1).

Tenchine, D., Barthel, V., Bieder, U., Ducros, F., Fauchet, G., Fournier, C., Mathieu, B., Perdu, F., Quemere, P., Vandroux, S., 2012. Status of TRIO_U code for sodium cooled fast reactors. Nuclear Engineering and Design 242, 307-315.

Tao, W.Q., 2001. Numerical heat transfer. Xi'an Jiaotong University Press, Xi'an.

Yue, N., Ma, Z., Cai, R., Hu, B., Su, G., Qiu, S., 2015. Thermal-hydraulic analysis of EBR-II Shutdown Heat Removal Tests SHRT-17 and SHRT-45R. Progress in Nuclear Energy 85, 682-693.